

# Titan's internal structure inferred from a coupled thermal-orbital model

Gabriel Tobie <sup>a,b,\*</sup>, Olivier Grasset <sup>b</sup>, Jonathan I. Lunine <sup>a</sup>, Antoine Mocquet <sup>b</sup>, Christophe Sotin <sup>b</sup>

<sup>a</sup> Lunar and Planetary Laboratory, University of Arizona, 1629 E University, P.O. Box 210092, Tucson, AZ 85721-0072, USA

<sup>b</sup> UMR 6112 Planétologie & Géodynamique, Faculté des Sciences, 44322 Nantes cedex 03, France

Received 3 August 2004; revised 18 November 2004

Available online 3 March 2005

## Abstract

Through coupled thermal and orbital calculations including a full description of tidal dissipation, heat transfer and the H<sub>2</sub>O–NH<sub>3</sub> phase diagram, we propose a model for the internal structure and composition of Titan testable with Cassini–Huygens measurements. The high value of Titan's orbital eccentricity provides a strong constraint on the amount of the tidal energy dissipation on its surface and within its interior since its formation. We show that only models with a few percent of ammonia (and not zero) in the primordial liquid water shell can limit the damping of the eccentricity over the age of the Solar System. The present models predict that a liquid ammonia-rich water layer should still be present within Titan under an ice I layer, a few tens of kilometers thick. Furthermore, we predict that any event linked to convective processes in the ice Ih layer (like the degassing of methane) could have occurred very late in Titan's history.

© 2005 Elsevier Inc. All rights reserved.

**Keywords:** Titan; Thermal histories; Ices; Tides, solid body; Orbits

## 1. Introduction

Titan, Saturn's largest moon, exhibits an orbital eccentricity several times higher than its jovian cousins Europa, Io and Ganymede. Frictional damping of tides raised by Saturn on Titan results in a progressive circularization of its eccentric orbit on a timescale determined by the energy dissipation rate. Previous computations of dissipation in a global surface hydrocarbon ocean (Sagan and Dermott, 1982; Sears, 1995) and/or within the interior (Sohl et al., 1995) indicated that, since no resonance with other Saturn satellites can force Titan's orbit and no recent major impact event is likely to have occurred (Sohl et al., 1995), its eccentricity should have been damped to a very small value compared to its current 3% value over the age of the Solar System, unless no global surface ocean exists and the interior is totally solid and volatile-poor. On the other hand, theoretical models of Titan's formation and evolution (Lunine and Stevenson, 1987; Stevenson, 1992; Grasset and Sotin, 1996;

Grasset et al., 2000; Sohl et al., 2003; Grasset and Pargamin, 2004) predict that a liquid water layer must exist below its icy surface, if a sufficient amount of ammonia is mixed with water. Ammonia within Titan is supported by accretion models (e.g., Mousis et al., 2002), by ammonia abundance in comets (e.g., Altwegg et al., 1994), and by the resurfacing of other saturnian satellites (e.g., Kargel and Pozio, 1996). It is known to limit the crystallization rate of the post-accretional liquid layer (Lunine and Stevenson, 1987; Kuramoto and Matsui, 1994) as the satellite cools down by lowering the crystallization point of water (Lunine and Stevenson, 1987; Grasset and Sotin, 1996). The internal structure would be then divided, from the surface to the center, into an ice Ih layer, an ammonia-rich water liquid layer, a high-pressure ice layer (phases V and VI), and a rocky core (Fig. 1). Predictions of liquid water layers within large icy satellites (Lunine and Stevenson, 1987; Grasset and Sotin, 1996; Deschamps and Sotin, 2001; Spohn and Schubert, 2003), supported for Ganymede and Callisto by Galileo magnetic data (Khurana et al., 1998; Kivelson et al., 2002), appears to conflict with Titan's high eccentricity (Sohl et al., 1995), since a subsurface liquid layer should increase the dissipa-

\* Corresponding author.

E-mail address: [gtobie@lpl.arizona.edu](mailto:gtobie@lpl.arizona.edu) (G. Tobie).

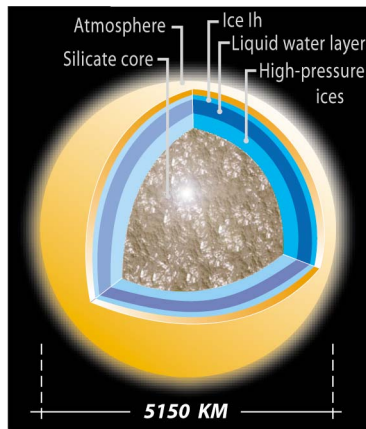


Fig. 1. Possible present-day structure of Titan's interior. The densities of the silicate interior, of the high-pressure layer, of the liquid water layer, and of the ice I layer are set to 3000, 1310, 1000, and 920  $\text{kg m}^{-3}$ , respectively. To verify the present-day value of Titan's density ( $\rho = 1881 \text{ kg m}^{-3}$ ), the silicate core radius is set to 1900 km and the total  $\text{H}_2\text{O}$  mass  $M_{\text{H}_2\text{O}}$  to  $4.82 \times 10^{22}$  kg.

tion rate in the outer ice Ih layer of the satellite. Furthermore, even though a current solid structure may satisfy the required low dissipative state of Titan's interior (Sohl et al., 1995), the evolution of dissipation during the freezing stage of the primordial outer liquid layer remains problematic.

These conflicting results may be reconcilable by studying how the existence of a liquid layer and its progressive freezing affect tidal dissipation and the decay of the orbital eccentricity. For this purpose, a coupled dynamical evolution model of Titan's orbit and interior has been set up. It performs a series of simulations from different initial states leading to Titan's current orbital configuration. The evolution is determined through self-consistent calculations of orbital evolution, tidal dissipation, heat transfer, and ocean crystallization. Though recent radar and IR measurements indicate the possible presence of hydrocarbon liquids on the surface of Titan (Campbell et al., 2003; Lellouch et al., 2004), we assume (consistent with near-infrared remote sensing of Lellouch et al. (2004)) the liquid to be in isolated basins so that it cannot contribute significantly to global dissipation (Dermott and Sagan, 1995) either by liquid-solid friction or by loading tides. We then assume that dissipation is only attributed to body tides inside solid and liquid layers of Titan's interior. Details of our coupled model are presented in Section 2. In Section 3, we first present some synthetic model results showing the effect of ammonia content on Titan's evolution, and we then discuss in more details one of our models. Finally, Section 4 provides some concluding remarks and implications for the Cassini–Huygens mission.

## 2. The model

The cooling rate of the liquid layer in Titan's interior depends on the amount of heat expelled from the satellite

through the outer ice Ih layer (e.g., Grasset and Sotin, 1996). Modeling the evolution of Titan's interior thus requires characterizing the amount of heat provided by the silicate core and by tidal dissipation, as well as the efficiency of heat transfer through the outer ice Ih layer and the phase diagram in the  $\text{NH}_3\text{--H}_2\text{O}$  system. In return, as the liquid layer crystallizes, the response of the satellite to tidal forcing evolves, modifying the amount of dissipated energy and its effect on heat transfer and on eccentricity decay.

Coupling between orbital and thermal evolution is achieved via tidal dissipation. At each time step in our model (fixed at  $10^5$  years), the tidal dissipation rate is calculated at each depth within the internal structure from the tidal potential imposed at Titan's surface, which depends on the orbital eccentricity  $e$  and the orbital frequency  $\omega$ , and from the temperature profile  $T(r)$ . The derived specific dissipation rate  $H_{\text{tide}}(r)$  is then used to deduce the heat fluxes at each interface and the evolution of the temperature profile. Due to the temperature dependence of the thermo-mechanical properties of ice Ih, we have developed a mutually consistent scheme to compute tidal dissipation and heat transfer through the outer ice Ih layer. The crystallization rate of the liquid layer is calculated from the heat fluxes at each interface, and new positions of the interfaces between the liquid layer and the ice layers (ice Ih layer and high-pressure ice layer) as well as the radius of the satellite are accordingly re-calculated after each time step. The evolution of orbital parameters is derived from the global dissipation rate, computed by integrating the specific dissipation rate  $H_{\text{tide}}(r)$  over the whole interior volume. Table 1 summarizes all the parameters defining our numerical model. We now proceed to the detailed presentation of each model component enumerated above.

### 2.1. Evolution of the silicate core

A fully differentiated structure as described in Fig. 1 is unlikely to exist just after Titan's accretion. More probably, a mixed ice-rock core may exist below a silicate mantle and an outer  $\text{H}_2\text{O}$  layer once its accretion is achieved (Kirk and Stevenson, 1987; Lunine and Stevenson, 1987). The complete segregation of ice and rock mixture within the core only occurs roughly one billion years after the accretion (Lunine and Stevenson, 1987). By simplicity, we start the evolution of Titan after the core overturn, assuming a partially hydrated silicate interior similar to model C of Sohl et al. (1995). Heat flow coming out of the silicate core is determined by both the amount of radiogenic elements and the efficiency of heat transfer. Tidal dissipation within the silicate interior is very low and can be neglected (Sohl et al., 2003; Sotin and Tobie, 2004). The early thermal evolution of a homogeneous chondritic core is characterized by a temperature increase controlled by diffusive heating, followed by marginal convection about 1 Ga after core overturn (Grasset et al., 2000). Then, the vigor of convection keeps increasing. Global heat coming out of the silicate core can

Table 1  
Physical parameters describing Titan's interior and orbit

	Parameter	Symbol	Unit	Value	Reference
<b>Orbit</b>	Saturn's mass	$M_S$	kg	$5.68 \times 10^{26}$	Sohl et al. (1995)
	Initial eccentricity	$e_0$		[0.04–0.4]	Free parameter
	Current eccentricity	$e_c$		0.0292	Sohl et al. (1995)
	Current semimajor axis	$a_c$	km	$1.2208 \times 10^6$	Sohl et al. (1995)
	Current frequency	$\omega_c$	rad s <sup>-1</sup>	$4.56 \times 10^{-6}$	Sohl et al. (1995)
<b>Internal structure</b>	Titan's mass	$M_T$	kg	$1.346 \times 10^{23}$	Sohl et al. (1995)
	Mass of silicate	$M_{\text{sil}}$	kg	$8.62 \times 10^{22}$	Sohl et al. (1995)
	Mass of H <sub>2</sub> O + NH <sub>3</sub>	$M_{\text{H}_2\text{O}-\text{NH}_3}$	kg	$4.84 \times 10^{22}$	Sohl et al. (1995)
	Ammonia mass fraction (= $M_{\text{NH}_3}/M_{\text{H}_2\text{O}-\text{NH}_3}$ )	$x_{\text{NH}_3}$	%	[0–8]	Free parameter
	Surface temperature	$T_s$	K	94	Sohl et al. (1995)
	Surface pressure	$P_s$	Pa	$1.5 \times 10^5$	Sohl et al. (1995)
<i>Interfaces</i>	Surface	$R_s$	km	Computed	
	Ice I/liquid	$R_{\text{I/O}}$	km	Computed	
	Liquid/HP ice	$R_{\text{O/HP}}$	km	Computed	
	HP ice/silicate	$R_{\text{sil}}$	km	1900	Sohl et al. (1995)
<i>Ice I</i>	Density	$\rho_{\text{I}}$	kg m <sup>-3</sup>	920	Sotin et al. (1998)
	S- and P-wave velocity	$V_S/V_P$	m s <sup>-1</sup>	1880/4000	Sotin et al. (1998)
	Thermal conductivity	$k_{\text{I}}$	W m <sup>-1</sup> K <sup>-1</sup>		Hillier and Squyres (1991)
	$k_{\text{I}}(T) = k_1/T + k_2$	$k_1/k_2$		488/0.4685	
	Heat capacity	$c_{\text{I}}$	J kg <sup>-1</sup> K <sup>-1</sup>		Hillier and Squyres (1991)
	$c_{\text{I}}(T) = c_1 T + c_2$	$c_1/c_2$		7.037/185	
	Latent heat of fusion	$L_{\text{I}}$	J kg <sup>-1</sup>	$284 \times 10^3$	Kirk and Stevenson (1987)
	Thermal expansion	$\alpha_{\text{I}}$	K <sup>-1</sup>	$1.56 \times 10^{-4}(T/250)$	Kirk and Stevenson (1987)
	Melting temperature				
	—of pure water ice	$T_m^0$	K	Computed	
	—in presence of ammonia	$T_m^{\text{NH}_3}$	K	Computed	
	Newtonian viscosity	$\eta_{\text{I}}$	Pa s	Eq. (1)	
Viscosity at $T = T_m^0$	$\eta_{m,0}$	Pa s	$[5.10^{13} - 5.10^{14}]$	Free parameter	
Activation energy	$E_a$	J mol <sup>-1</sup>	$50 \times 10^3$	Tobie et al. (2003)	
<i>Liquid water</i>	Density	$\rho_w$	kg m <sup>-3</sup>	1000	
	S- and P-wave velocity	$V_S/V_P$	m s <sup>-1</sup>	0/1500	Tobie et al. (2003)
	Heat capacity	$c_w$	J kg <sup>-1</sup> K <sup>-1</sup>	4180	Kirk and Stevenson (1987)
	Thermal expansion	$a_w$	K <sup>-1</sup>	$3 \times 10^{-4}$	Grasset et al. (2000)
<i>High pressure ice</i>	Density	$\rho_w$	kg m <sup>-3</sup>	1310	Grasset et al. (2000)
	S- and P-wave velocity	$V_S/V_P$	m s <sup>-1</sup>	1880/4000	Sotin et al. (1998)
	Latent heat of fusion	$L_{\text{HP}}$	J kg <sup>-1</sup>	$294 \times 10^3$	Kirk and Stevenson (1987)
	Heat capacity	$c_{\text{HP}}$	J kg <sup>-1</sup> K <sup>-1</sup>	1925	Kirk and Stevenson (1987)
<i>Silicate</i>	Density	$\rho_{\text{sil}}$	kg m <sup>-3</sup>	3000	Sohl et al. (1995)
	Newtonian viscosity	$\eta_{\text{sil}}$	Pa s	$10^{20}$	Tobie et al. (2003)
	S- and P-wave velocity	$V_S/V_P$	m s <sup>-1</sup>	4500/8000	Tobie et al. (2003)
	Radiogenic heating	$H_0$	W kg <sup>-1</sup>	$4 \times 10^{-11}$	Deschamps and Sotin (2001)
	Decay constant	$\lambda$	s <sup>-1</sup>	$1.38 \times 10^{-17}$	Deschamps and Sotin (2001)
	Heat flux out of the silicate core	$\Phi_{\text{sil}}$	W m <sup>-2</sup>	Computed	after (Grasset et al., 2000)

be as high as 600 GW (Tobie, 2003) at the present time, including contributions of both radiogenic decay and secular cooling.

## 2.2. Tidal dissipation and orbit evolution

The body tide dissipation is calculated by integrating the equations of motions and Poisson's equation from the center of the satellite to its surface, and by imposing the tide-generating potential induced by Saturn at the surface (Tobie

et al., in preparation). Assuming a compressible Maxwell rheology, the viscoelastic properties of each layer are defined from the values of the elastic S- and P-wave velocities,  $V_S$  and  $V_P$ , respectively, and the effective Newtonian viscosity  $\eta$  (see Table 1). The elastic shear and bulk moduli,  $\mu_E$  and  $K_E$  respectively are related to the S- and P-wave velocities (listed in Table 1 for each internal layer) by the following relationship:  $\mu_E = \rho V_S^2$ , and  $K_E = \rho V_P^2 - 4/3\mu_E$ . Temperature dependent viscosity of ice Ih is evaluated from the homologous temperature  $T/T_m^0$  (e.g., Kirk and Steven-

son, 1987):

$$\eta(T) = \eta_{m,0} \exp\left(\frac{E_a}{RT_m^0} [T_m^0/T - 1]\right), \quad (1)$$

where  $T_m^0$  is the melting temperature of pure water ice Ih,  $\eta_{m,0}$  is the viscosity of pure ice Ih at the melting point, and  $E_a$  is the activation energy (see Table 1). By simplicity, the same formulation is used for the temperature dependence of high-pressure ices, and the homologous temperature  $T/T_m^0$  is assumed constant through the high-pressure ice layer. For the numerical computation of Titan's radial functions (see Tobie et al., in preparation), the outer ice Ih layer is divided in five sublayers in the conductive part and ten sublayers in the convective part, both the liquid layer and the high-pressure layer are divided in ten sublayers. One hundred sublayers are used to resolve the temperature profile in the diffusive part of the ice Ih layer and the homologous  $T/T_m$  is assumed constant through the convective part. The radial functions of the satellite are not re-computed at each time step, but only when the cumulative radius variations at all interfaces, as defined in Table 1, exceed 10 km.

The global dissipation rate  $dE/dt$  is computed by integrating the specific dissipation rate  $H_{\text{tide}}$  calculated in each layer of the model. From the global tidal dissipation rate  $dE/dt$ , the temporal evolution of Titan's orbital parameters is assessed using the conservation of angular momentum under the assumption of orbital synchronicity. Peale (1977) showed that even if Titan spun rapidly after its accretion, tides raised on the satellite by Saturn must have slowed down its rotation toward synchronicity before core overturn was achieved ( $t < 1$  Ga). Then, the loss of Titan's orbital energy manifests as a reduction in orbital eccentricity (Sears, 1995), and the change in eccentricity due to tidal dissipation is given by (Sohl et al., 1995):

$$\frac{de}{dt} \frac{e}{1-e^2} = \frac{-a}{GM_S M_T} \frac{dE}{dt}, \quad (2)$$

where  $M_S$  and  $M_T$  are the mass of Saturn and Titan, respectively,  $e$  is the eccentricity,  $a$  is the semimajor axis of the orbit. In addition, the conservation of orbital angular momentum implies:  $a(1-e^2) = a_c(1-e_c^2) = a_0(1-e_0^2)$ . The indices 0 and c refer to the initial and current state, respectively. This formulation does not take into account the tidal expansion of Titan's orbit due to dissipation of tides raised by Titan on Saturn. However, for realistic values of dissipation factors,  $Q_T$  and  $Q_S$ , within Titan and Saturn ( $Q_T < 500$  (this study) and  $Q_S > 10^4$  (Peale, 1999)), the effect of dissipation within Saturn corresponds to less than 2% of the effect of dissipation within Titan on the eccentricity variation, and therefore can be safely neglected.

### 2.3. Heat transfer through the ice Ih layer

Heat can be transferred either by thermal diffusion or convection, depending on ice Ih layer thickness and on ice Ih viscosity. In both cases, the temperature dependence of

both ice Ih viscosity (Eq. (1)) and thermal diffusivity (Table 1) as well as the viscosity dependence of tidal dissipation (Tobie et al., 2003) are included in our calculations. The ice Ih layer becomes convective when the Rayleigh number associated with the layer exceeds the critical value as defined by Stengel et al. (1982). The Rayleigh number is defined as  $Ra = \alpha_I \rho_I g \Delta T b^3 / \kappa_I \eta_I$ , with  $\alpha_I$ , ice I thermal expansion,  $\rho_I$ , ice I density,  $g$  acceleration of gravity,  $\Delta T$  temperature variation between the base and the top of the ice Ih layer,  $b$ , ice Ih layer thickness,  $\kappa_I (= k_I / \rho_I c_I)$  ice Ih thermal diffusivity,  $\eta_I$  ice Ih viscosity. All these parameters are estimated for the temperature of the well-mixed convective sublayer. The temperature profile in the ice Ih diffusive layer is computed by solving the diffusion equation including tidal dissipation and temperature-dependent ice Ih diffusivity with a Crank–Nicholson scheme. With bodies whose outer layers are made of water ice, thermal convection occurs in the stagnant lid regime (e.g., Deschamps and Sotin, 2001). The upper part of the ice Ih layer remains diffusive, convective motions and dissipation are confined to a quasi-isoviscous, well-mixed, sublayer (e.g., McKinnon, 1999). Relationships between heat fluxes and temperature differences across the thermal boundary layers are controlled by viscously-determined scales and Rayleigh number of the whole ice Ih layer (Grasset and Parmentier, 1998; Dumoulin et al., 1999; Deschamps and Sotin, 2001; Tobie, 2003), and are constrained from numerical experiments of thermal convection including viscosity-dependent tidal heating (Tobie et al., 2003; Tobie, 2003). Heat fluxes at the base and at the top of both convective and conductive ice Ih sublayers, as well as internal heating due to tidal dissipation in the convective sublayer control the evolution of both the temperature of the well-mixed convective sublayer and of the thickness of the overlying conductive lid. For this purpose, we use the formulation proposed by Schubert and Spohn (1990).

### 2.4. Crystallization of the liquid layer

Following Grasset and Sotin (1996), the rate of ocean crystallization is determined using the heat flux values obtained at the base of the ice Ih layer and at the top of the high-pressure ice layer (i.e., heat flow from the silicate core—due mainly to the radiogenic decay of isotopic elements—plus tidal dissipation in the high-pressure ice layer). The temperature evolution of each solid/liquid interface during the ocean crystallization, and the increase of ammonia concentration  $C_{\text{NH}_3}^w = M_{\text{NH}_3} / M_{\text{liquid}}$  in the liquid layer, where  $M_{\text{NH}_3}$  and  $M_{\text{liquid}}$  are the mass of ammonia and the mass of the liquid layer respectively, are calculated accurately using a new algorithm describing the liquidus in the  $\text{H}_2\text{O}$ – $\text{NH}_3$  system (Grasset and Pargamin, 2004). The values of gravity and pressure, the adiabatic temperature profile in the ocean, and the equilibrium temperature at each ice-ocean interface, all required to derive the thickening rate of both the outer ice Ih layer and the high-pressure ice layer, are calculated by in-

tegrating the differential equations for mass, acceleration of gravity and pressure (e.g., Sohl et al., 2002). The radius of Titan is not prescribed and is re-calculated at each time step in our evolution model, as the ice layers crystallize. Only the global mass of silicate, water and ammonia are prescribed in our model. The accurate calculation of the temperature evolution at the interface ocean-ice Ih is fundamental, considering the strong coupling between heat transfer and tidal dissipation via the temperature dependence of ice Ih viscosity.

### 3. Results and discussion

Starting from different sets of initial eccentricity  $e_0$  and global ammonia mass fraction  $x_{\text{NH}_3}$  ( $M_{\text{NH}_3}/M_{\text{H}_2\text{O-NH}_3}$ ), we investigate the long-term evolution of Titan's interior from one billion years to the present, and derive the interior models compatible with its present-day orbital configuration. After one billion years, the formation of a silicate core can be reasonably considered to have been achieved (Lunine and Stevenson, 1987), and the energy contribution due to meteoritic bombardment can be safely neglected. Figure 2 summarizes the initial eccentricity value  $e_0$  that leads to the current orbital configuration, and the current thickness  $b_{\text{liq}}$  of the liquid layer, as a function of the ammonia mass fraction  $x_{\text{NH}_3}$ , for four different viscosity values of ice Ih near the melting point. Whatever the values of ammonia mass fraction and of ice Ih viscosity at the melting point, the current configuration can be explained if the initial eccentricity is at least higher than 0.08. The present-day equilibrium state

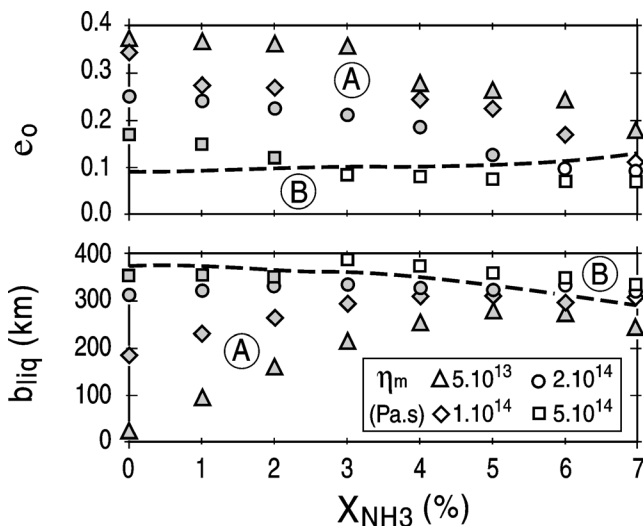


Fig. 2. Initial eccentricity values  $e_0$  at  $t_0 = 1$  Ga explaining present-day Titan's orbit configuration (upper graph), and current thickness  $b_{\text{liq}}$  of the liquid layer as a function of global ammonia mass fraction  $x_{\text{NH}_3}$ , for different values  $\eta_m$  of ice Ih viscosity near the melting point. The viscosity of high-pressure ice at the melting point is prescribed to be  $10^{14}$  Pa.s. Domains A and B delineated by dashed lines, correspond to different (convective and/or conductive) thermal regimes in the outer ice I layer (see text for details).

always includes a deep liquid layer ranging from a few kilometers to almost four hundred kilometers in thickness, depending on the ice Ih viscosity value and on the ammonia mass fraction.

The present-day ocean is overlain by a convective (domain A in Fig. 2) or diffusive (domain B in Fig. 2) ice Ih shell. For lowest viscosity values and lowest ammonia fractions (domain A), higher initial eccentricity values are required, because the ice Ih shell becomes convective and highly dissipative some time during Titan's evolution. The later convection in the outer ice Ih layer starts, the smaller the required initial eccentricity is. For the highest viscosity values and/or highest ammonia fractions (domain B), convection never initiates. The ice Ih layer remains diffusive and low dissipative up to present time. Initial eccentricities lower than 0.1 can explain the current state.

An interesting point is that the evolution path leading to a complete freezing of the primordial liquid layer (not shown on Fig. 2), which is achieved for low viscosity values and no ammonia, always results in a complete damping of the initial eccentricity, at least for values lower than 0.3–0.4. Our results indicate that, if Titan's current interior is totally solid, it has always been in this state, which would give strong constraints on the processes of Titan's formation (Kuramoto and Matsui, 1994). Conversely, if a primordial liquid layer was formed during the accretion, it should be still present below the icy surface and may contain a significant fraction of ammonia.

A major issue concerns the plausible value of the initial eccentricity. Different processes, such as gravitational interactions between proto-Titan and Saturn's gas disk (Goldreich and Tremaine, 1980) or impact with another big satellite "embryo" (Mosqueira and Estrada, 2003), may strongly excite the primordial eccentricity during Titan's accretion. Recent discoveries of exoplanets with large orbital eccentricity have modified our understanding of planetary system formation and have contradicted, especially in the case of isolated planet, the view that planet (or satellite)–disk interactions damp eccentricities (e.g., Artymowicz, 1993). Goldreich and Sari (2003) recently show that Lindblad resonances would be able to overcome the damping interaction processes and significantly excite the orbital eccentricity if the planetary body opens a gap within the gas disk. Within Saturn's subnebula, proto-Titan should have been massive enough to induce a gap opening and control the further evolution of the disk (Mosqueira and Estrada, 2003). Even though eccentricity values as high as 0.3–0.4 may have been resulted from this process, the 4:3 resonance of Hyperion and Titan and their proximity remains quite puzzling in such a context.

One possibility is that the orbital resonance took place as Hyperion formed (Lee and Peale, 2000), rather than as a consequence of tidal expansion of Titan's orbit, which requires unrealistic dissipation within Saturn and Titan (Peale, 1999). However, the feasibility of concomitant Hyperion formation and resonance capture when Titan had a high eccentricity is

yet to be demonstrated. Furthermore, the proximity of Hyperion ( $a_H = 1.481 \times 10^6$  km,  $a_T = 1.221 \times 10^6$  km) provides direct constraints on the initial position of Titan with respect to Hyperion (Sears, 1995). From the conservation of angular momentum, it can be showed that Titan's orbit would cross Hyperion's current one if Titan's eccentricity  $e_T$  is higher than 0.09. Nevertheless, the past orbit of Hyperion may have been quite different from its current configuration. Assuming that the 4:3 Hyperion–Titan resonance is primordial and the couple has evolved in deep resonance, one can expect that close encounter of the two satellites would be avoided as long as  $e_T < 0.15$ – $0.2$ , because the distance of closest approaches would be maximized (e.g., Peale, 1999). Nevertheless, whatever the initial values of eccentricity, the stability of Hyperion–Titan resonance remains problematic as Titan moves inward. The complexity of the problem even increases if one considers that past Hyperion was more massive, as suggested by its irregular shape (Farinella et al., 1983). Future theoretical investigations on this problem are required to give more precise constraints on the initial eccentricity. In summary, although there are no real upper limits on the primordial eccentricity as a result of accretion process, eccentricities higher than 0.1–0.2 seem very difficult to reconcile with Hyperion's proximity.

For an upper bound of 0.2 for the primordial eccentricity and ice Ih viscosity values around  $10^{14}$  Pa s at the melting point, a few percent of ammonia is required to satisfy the current eccentricity. For a 6% ammonia mass fraction (Fig. 3), a thick ( $\sim 300$  km, Fig. 2) deep liquid layer with 14 wt% ammonia may still exist below an ice Ih shell thinner

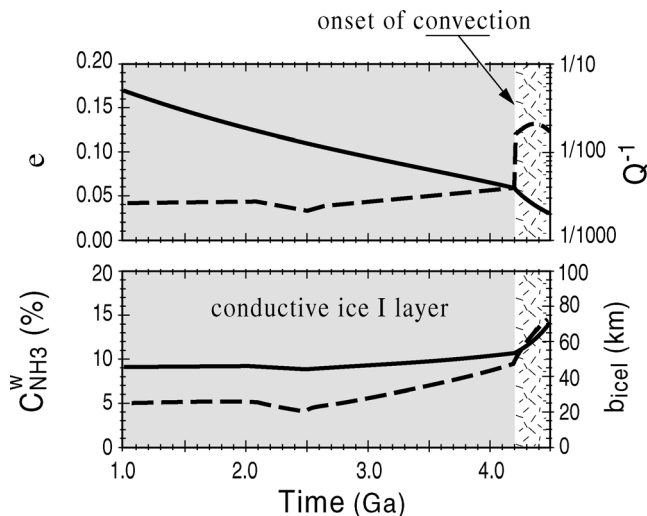


Fig. 3. Temporal evolution of orbital eccentricity  $e$  (solid curve), of global dissipation function  $Q^{-1}$  (dashed curve), of ammonia concentration in the water layer  $C_{\text{NH}_3}^w$  (solid curve) and, of ice Ih layer thickness  $b_{\text{iceI}}$  (dashed curve), for ammonia mass fraction value of 6% and a viscosity value at the melting point equal to  $10^{14}$  Pa s for both high-pressure ice and ice Ih. Note that convection starts in the outer ice Ih layer around  $t = 4.2$  Ga, inducing an increase of both dissipation and crystallization rate. The decrease of the ice Ih layer thickness between 2 and 2.5 Ga is related to the onset of convection in the silicate core at 2 Ga with a maximum of convective heat flux at 2.5 Ga (Grasset et al., 2000).

than 75 km in agreement with Sohl et al. (2003). The global dissipation function  $Q^{-1}$ , which is proportional to the dissipation rate, evolves with time, being lower than  $1/300$  as long as the ice Ih layer is conductive and increasing abruptly above  $1/100$  once convection starts ( $t \sim 4.2$  Ga). The principal effect of ammonia is to delay the onset of convection and to keep the interior in a low dissipative state ( $Q^{-1} < 1/300$ ) during the major part of Titan's history, if not during its whole history. We have investigated the effect of different amount of radiogenic heating in the silicate core and a range of values for viscosity of high-pressure phases of ice. These effects are second order compared to the effect of ammonia.

#### 4. Concluding remarks

The most realistic models ( $e_0 < 0.2$ ) predict that the outer ice Ih layer above a water ocean with more or less ammonia fraction depending on the viscosity value  $\eta_m$ , could have been as thin as 20–25 km in the past when the eccentricity was higher and the ice Ih layer was conductive, as illustrated on Fig. 3. If Titan's atmospheric methane is renewed by degassing due to release of methane clathrate hydrate stored into the deep interior (Loveday et al., 2001) and transported by thermal convection through the ice Ih layer, our model predicts that such a process occurred very late in Titan's history and required an initial eccentricity higher than 0.1. Before the onset of convection on Fig. 3 ( $t < 4.2$  Ga), the eccentricity is several times higher than its present-day value. Such a high value produces tidal stresses and tidal dissipation of the same magnitude than what Europa is currently experiencing (e.g., Tobie et al., 2003). One can expect that Titan was, and maybe still is, subject to active tectonic processes.

Orbit tracking of the Cassini spacecraft as it flies past Titan during the latter's periapse and apoapse around Saturn may provide detection of an interior liquid mantle (Castillo et al., 2002). The presence of an induced magnetic field could also be indicative of such a layer, though the much weaker saturnian magnetic field compared to Jupiter's as well ionospheric interactions may make this test difficult (Khurana et al., 1998; Neubauer et al., 2003). The Visible and Infrared Mapping Spectrometer, CRS (Cassini Radar System) and ISS (Imaging Science Subsystem) instruments on the Cassini orbiter are capable of revealing tectonic features that can constrain the models of Titan's history developed in the present paper.

#### Acknowledgments

The image of Titan's interior (Fig. 1) has been realized by Alain Cossard at the Laboratoire de Planétologie & Géodynamique (Nantes, Fr). The research was done while G.T. was a visiting scholar at the LPL, partially supported by a Lavoisier fellowship from the French government. J.L. is

grateful to the Cassini Project for additional support. We thank Frank Sohl for his constructive review, as well as Daniel Gautier, Ralph Lorenz, Renu Malhotra, Giuseppe Mitri, Ignacio Mosqueira, Adam Showman, and Alain Vi-  
enne for interesting discussions.

## References

- Altwegg, K., Balsiger, H., Geiss, H., 1994. Abundance and origin of the  $\text{CH}_4^+$  ions in the coma of Comet P/Halley. *Astron. Astrophys.* 290, 318–323.
- Artymowicz, P., 1993. Disk–satellite interaction via density waves and the eccentricity evolution of bodies embedded in disks. *Astrophys. J.* 419, 166–180.
- Campbell, D.B., Black, G.J., Carter, L.M., Ostro, S.J., 2003. Radar evidence for liquid surfaces on Titan. *Science* 302, 431–434.
- Castillo, J., Rappaport, N., Mocquet, A., Sotin, C., 2002. Clues on Titan's internal structure from Cassini–Huygens mission. *Lunar Planet. Sci.* 33. Abstract 1989.
- Dermott, S.F., Sagan, C., 1995. Tidal effects of disconnected hydrocarbon seas on Titan. *Nature* 374, 238–240.
- Deschamps, F., Sotin, C., 2001. Thermal convection in the outer shell of large icy satellites. *J. Geophys. Res.* 106, 5107–5121.
- Dumoulin, C., Doin, M., Fleitout, L., 1999. Heat transport in stagnant lid convection with temperature- and pressure-dependent Newtonian or non-Newtonian rheology. *J. Geophys. Res.* 104, 12759–12778.
- Farinella, P., Milani, A., Nobili, A.M., Paolicchi, P., Zappala, V., 1983. Hyperion—collisional disruption of a resonant satellite. *Icarus* 54, 353–360.
- Goldreich, P., Sari, R., 2003. Eccentricity evolution for planets in gaseous disks. *Astrophys. J.* 585, 1024–1037.
- Goldreich, P., Tremaine, S., 1980. Disk–satellite interactions. *Astrophys. J.* 241, 425–441.
- Grasset, O., Pargamin, J., 2004. The ammonia water system at high pressures: implications for the methane of Titan. *Planet. Space Sci.* In press.
- Grasset, O., Parmentier, E.M., 1998. Thermal convection in a volumetrically heated, infinite Prandtl number fluid with strongly temperature-dependent viscosity: implications for planetary evolution. *J. Geophys. Res.* 103, 18171–18181.
- Grasset, O., Sotin, C., 1996. The cooling rate of a liquid shell in Titan's interior. *Icarus* 123, 101–112.
- Grasset, O., Sotin, C., Deschamps, F., 2000. On the internal structure and dynamics of Titan. *Planet. Space Sci.* 48, 617–636.
- Hillier, J., Squyres, S.W., 1991. Thermal stress tectonics on the satellites of Saturn and Uranus. *J. Geophys. Res.* 96, 15665–15674.
- Kargel, J.S., Pozio, S., 1996. The volcanic and tectonic history of Enceladus. *Icarus* 119, 385–404.
- Khurana, K.K., Kivelson, M.G., Russel, C.T., 1998. Induced magnetic field as evidence for subsurface oceans in Europa and Callisto. *Nature* 397, 777–780.
- Kirk, R.L., Stevenson, D.J., 1987. Thermal evolution of a differentiated Ganymede and implications for surface features. *Icarus* 69, 91–134.
- Kivelson, M.G., Khurana, K.K., Volwerk, M., 2002. The permanent and inductive magnetic moments of Ganymede. *Icarus* 157, 507–522.
- Kuramoto, K., Matsui, T., 1994. Formation of a hot proto-atmosphere on the accreting giant icy satellite: implications for the origin and evolution of Titan, Ganymede, and Callisto. *J. Geophys. Res.* 99 (E10), 21183–21200.
- Lellouch, E., Schmitt, B., Coustenis, A., Cuby, J.G., 2004. Titan's 5-micron lightcurve. *Icarus* 168, 209–214.
- Lee, M.H., Peale, S.J., 2000. The puzzle of the Titan–Hyperion 4:3 orbital resonance. *Bull. Am. Astron. Soc.* 32, 860.
- Loveday, J.S., Nelmes, R.J., Guthrie, M., Belmonte, S.A., Allan, D.R., Klug, D.D., Tse, J.S., Handa, Y.P., 2001. Stable methane hydrate above 2 GPa and the source of Titan's atmospheric methane. *Nature* 410, 661–663.
- Lunine, J.I., Stevenson, D.J., 1987. Clathrate and ammonia hydrates at high pressure—application to the origin of methane on Titan. *Icarus* 70, 61–77.
- McKinnon, W.B., 1999. Convective instability in Europa's floating ice shell. *Geophys. Res. Lett.* 26, 951–954.
- Mosqueira, I., Estrada, P.R., 2003. Formation of the regular satellites of giant planets in an extended gaseous nebula II: satellite migration and survival. *Icarus* 163, 232–255.
- Mouis, O., Gautier, D., Bockelée-Morvan, D., 2002. An evolutionary turbulent model of Saturn's subnebula: implications for the origin of the atmosphere of Titan. *Icarus* 156, 162–175.
- Neubauer, F.M., Schilling, N., Backes, H., 2003. Electromagnetic sounding of Titan's interior in search of an ocean using magnetic field measurements during close encounters. In: AAS/DPS Meeting #35. #21.06.
- Peale, S.J., 1977. Rotation histories of the natural satellites. In: Burns, J.A. (Ed.), *Planetary Satellites*. Univ. of Arizona Press, Tucson, pp. 87–111.
- Peale, S.J., 1999. Origin and evolution of the natural satellites. *Annu. Rev. Astron. Astrophys.* 37, 533–602.
- Sagan, C., Dermott, S.F., 1982. The tide in the seas of Titan. *Nature* 300, 731–733.
- Schubert, G., Spohn, T., 1990. Thermal history of Mars and the sulfur content of its core. *J. Geophys. Res.* 95, 14095–14104.
- Sears, W.D., 1995. Tidal dissipation in oceans on Titan. *Icarus* 113, 39–56.
- Sohl, F., Sears, W.D., Lorenz, R.D., 1995. Tidal dissipation on Titan. *Icarus* 115, 278–294.
- Sohl, F., Spohn, T., Breuer, D., Nagel, K., 2002. Implications from Galileo observations on the interior structure and chemistry of the Galilean satellites. *Icarus* 157, 104–119.
- Sohl, F., Hussmann, H., Schwentker, B., Spohn, T., Lorenz, R.D., 2003. Interior structure models and tidal Love numbers of Titan. *J. Geophys. Res.* 108 (E12). CiteID 5130.
- Sotin, C., Tobie, G., 2004. Internal structure and dynamics of the large icy satellites. *C. R. Phys.* 5, 769–780.
- Sotin, C., Grasset, O., Beauchesne, S., 1998. Thermodynamical properties of high pressure ices: implications for the dynamics and internal structure of large icy satellites. In: Schmitt, B., De Bergh, M., Festou, C. (Eds.), *Solar System Ices*. Kluwer Academic, Dordrecht, the Netherlands, pp. 79–96.
- Spohn, T., Schubert, G., 2003. Oceans in the icy satellites of Jupiter? *Icarus* 161, 456–467.
- Stengel, K.C., Oliver, D.C., Booker, J.R., 1982. Onset of convection in a variable viscosity fluid. *J. Fluid Mech.* 120, 411–431.
- Stevenson, D.J., 1992. Interior of Titan. In: *Proceedings Symposium on Titan*, Toulouse, France, 9–12 September 1991. European Space Agency, Noordwijk, the Netherlands, pp. 29–33.
- Tobie, G., 2003. Impact of tidal heating on the geodynamical evolution of Europa and Titan. PhD thesis. University of Paris, France.
- Tobie, G., Choblet, C., Sotin, C., 2003. Tidally heated convection: constraints on Europa's ice shell thickness. *J. Geophys. Res.* 108 (E11). CiteID 5124.